

Desalination using Graphene Oxide-Cellulose Composite Membrane

Abstract

Ion separation potential of graphene oxide-cellulose membrane produced from waste materials for use in filtration processes is demonstrated in this study. Graphene nanomaterial was prepared by electrochemical exfoliation of electrodes from waste zinc-carbon batteries, and characterized using TEM, UV-Vis, FTIR, and SEM/EDX techniques. The membrane was fabricated from graphene oxide and recycled cellulose paper pulp and was also characterized. The membrane has a surface area of 0.001735 m^2 , and under vacuum pressure of 0.3 Pa was found to have average permeability of $6.5285 \times 10^{-5} \text{ m}^3/\text{m}^2 \cdot \text{s} \cdot \text{Pa}$, flux of $1.9585 \times 10^{-5} \text{ m}^3/\text{m}^2 \cdot \text{s}$, and volumetric flow rate of $3.3985 \times 10^{-6} \text{ m}^3/\text{s}$. Membrane desalination studies were performed using suction pump set-up for time intervals of 30, 60, 90, 120, and 150 min on sodium chloride – simulated brackish, saline and hyper-saline water. The ion separation efficiency measured by conductivities of water samples was found at the end of 150 min to be 91.0, 90.89, and 92.98% for brackish, saline, and hyper-saline water respectively. Optimum ion separation was obtained in the first 30 min of desalination experiment (96.95, 96.63 and 96.56% for brackish, saline, and hyper-saline water respectively), after which there was progressive increase in conductivities of all water samples due to swelling of the composite membrane.

Keywords: Desalination, Membrane, Recycled cellulose paper, Graphene nanomaterials, Electrochemical exfoliation

INTRODUCTION

An estimated one billion people in the world lack access to clean drinking water and the water scarcity is continually worsened by water contamination and overuse due to human activities (Zhong *et al.*, 2020). As a result, there have been persistent efforts at addressing the global water challenge, including the development of improved technologies for water treatment, recycling and reuse (Chen *et al.*, 2020; Zhong *et al.*, 2020). In the options, desalination of the abundant seawater resource has been considered as a promising technology that could meet the current fresh water demands, with the global desalination capacity standing at about 90 million m³ (Anis *et al.*, 2019). Majorly, desalination is achieved by thermal or membrane processes. The membrane technology in water desalination has the advantages of high efficiency, low energy consumption, and low environmental impacts (Song *et al.*, 2018). Membranes have been well researched, but the need to meet new desalination requirements has necessitated the development of various types of functional materials that would enhance the performance of desalination membranes (Teow and Mohammad, 2017). The choice of functional materials such as zeolites, carbon nanotubes, graphene nanomaterials, etc. depends on their role in membrane performance.

Several studies have shown that graphene oxide membranes show great potential in molecular separation for water especially as shown using desalination membrane of graphene oxide with mixed cellulose support treatment (Song *et al.*, 2018; Chen *et al.*, 2020; Zhong *et al.*, 2020). Also, the efficient removal of small molecules using cellulose-graphene quantum dot composite membranes has been reported (Colburn *et al.*, 2018). The graphene-based materials have excellent advantages in the membrane desalination process due to their intriguing features, including single atomic layer structure, large specific surface area, hydrophobic property, rich modification approaches, and more (Song *et al.*, 2018). However, graphene-based membranes

suffer from the problem of graphene synthesis, instability in water with uncertain permeance and the ease to detach from the support membranes during the separation process (Anis *et al.*, 2019). The water permeation through graphene oxide membranes is a key for its promising potential for filtration and purification applications whereas the reported water fluxes of graphene oxide membranes vary greatly in different literatures (Zhang *et al.*, 2020).

The mass production of graphene oxide and graphene nanomaterials for membrane application is also faced with challenges in meeting the application requirements (Anis *et al.*, 2019). Different graphene/graphene oxide preparation methods have been developed including mechanical exfoliation and epitaxial growth (Su *et al.*, 2011), chemical vapor deposition (Lin *et al.*, 2018), chemical exfoliation by Hummer's method and its modified forms (Hayes *et al.*, 2014), and electrochemical exfoliation (Su *et al.*, 2011) among others. The electrochemical exfoliation method has attracted attention due to its easy, fast, and environmentally friendly nature to produce high-quality graphene (Sahoo *et al.*, 2020).

Although there have been major improvements in recycling of used paper materials over the last decades, the pulp and paper sector remains a leading contributor to global greenhouse gas emissions, nitrogen pollution, and other environmental pressures (Chen *et al.*, 2020). It was reported that the world consumption of paper in 2019 exceeded 400 million tons per year (Ezeudu *et al.*, 2019). In the United States alone, paper and paperboard accounted for over 27 percent of the 251 million tons of total municipal solid waste generation in 2013 (Abdel-Shafy and Mansour 2018). More recently, it was projected that the global waste generation would increase to 3,539 megatons by 2050 from its 2015 total of 1,999 megatons. In the forecast, the global share of paper waste is particularly expected to increase from 2015 to 2050 (Chen *et al.*, 2020), thereby threatening the united nation sustainable development goals (UN SDGs).

In the present study, graphene oxide was produced by electrochemical exfoliation of zinc-carbon electrodes of used batteries. The graphene oxide membrane was then prepared by incorporating graphene oxide into recycled waste cellulose paper as membrane support. The graphene nanomaterial and membrane prepared were characterized using TEM, UV-Vis, FTIR, and SEM/EDX techniques. The ion separation efficiency of the produced graphene oxide membrane was investigated using sodium chloride – simulated brackish, saline and hyper-saline water.

METHODOLOGY

Materials

The materials and chemicals used for this research work include potassium chlorate, hydrochloric acid, sodium chloride, distilled water, deionized water, filter papers, S-PAK filter, waste newspaper, and sodium chloride. The waste zinc-carbon batteries (ZCBs) were gotten from various discharged batteries found in Ilorin metropolis. Apparatus and equipment used are alligator clips, connecting cables, ammeter, voltmeter, voltage supply source, suction pump, Buchner funnel, centrifuge, suction pump set-up, and electrical conductivity (EC) meter.

Preparation and Characterization of Graphene/Graphene Oxide

Zinc-carbon electrodes taken out of discharged ZCBs were washed with the dilute hydrochloric acid, and boiled in ultrapure deionized water for about 5 minutes to remove the residual impurities. The electrodes were subjected to electrochemical exfoliation for synthesis of graphene/graphene oxide nanomaterials. Electrochemical exfoliation experiments were performed in potassium chlorate at room temperature with voltage supplied by a laboratory DC power supply (MCP Model: M10-SP3003L). It was carried out at voltage values of 6.0, 7.5, 9.0, 10.5, and 12.0 V over five hours. At the completion of electrochemical exfoliation, the sample mixture was

centrifuged at 4000 rpm for 10 min to form a fine suspension. The suspension was then deposited on a filter paper by using a Büchner funnel and the residue on filter paper was washed with 100 ml of distilled water. The solid obtained was allowed to dry at room temperature and weighed to determine the product yield. The graphene nanomaterial was characterized by transmission electron microscopy (TEM), high resolution scanning electron microscopy/energy dispersive X-ray analysis (HRSEM/EDX), ultraviolet-visible (UV-Vis) spectroscopy, and Fourier transform infrared (FTIR) analysis.

Preparation of the Graphene Membrane

The graphene membrane was prepared according to procedure described in Koga *et al.* (2016). An aqueous suspension of cellulose pulp fibers that consist of recycled waste pulps from newspapers (0.15 wt%, 200 mL) was mixed with aqueous dispersion of graphene material that was produced via electrochemical exfoliation of discharged battery. An aqueous solution of polyvinyl alcohol (PVA) (1.0 wt%, 0.4 mL) was added at intervals of 10 minutes to the solution. The resultant solution was filtered by suction filtration using Büchner funnel through a supported membrane (S-PAK filter). Thereafter, the wet paper sample was hot pressed at 110 °C for 10 minutes to dry the sample. The graphene membrane was later used for desalination experiments

Properties of Graphene Membrane

The membrane morphology was examined using high resolution scanning electron microscopy (HRSEM), and energy dispersive X-ray (SEM/EDX) analysis. The swelling ratio of the membrane was obtained by immersing the membrane in deionized water for 6 hr. Then, excess water on the membrane was wiped with tissue paper and the wet membrane was weighed (M_{wet}). Thereafter the membrane was fully dried at room temperature and weighed again (M_{dry}). The swelling property of the membrane was determined using Equation (1);

$$\text{Swelling ratio} = \frac{M_{\text{wet}} - M_{\text{dry}}}{M_{\text{dry}}} \times 100 \quad (1)$$

Other membrane properties which include surface area (A), volumetric flow rate (G), flux (\dot{G}), and permeability (μ) were calculated using Equations (2) – (5), where r is radius of the circular membrane, $\pi = 3.142$, and p is the suction pressure.

$$A = \pi r^2 \quad (2)$$

$$G = \frac{V}{t} \quad (3)$$

$$\dot{G} = \frac{G}{\pi r^2} \quad (4)$$

$$\mu = \frac{G}{\pi r^2 p} \quad (5)$$

Desalination Experiment

Three forms of saline water were considered in this study; brackish water, saline water, and hyper saline water. Simulated salt water was prepared by measuring 20 g, 35 g, or 50 g of sodium chloride in a beaker and adding fresh water to it until the total mass of the salt and water weighed 1 kg to form brackish, saline, or hyper-saline water respectively. The conductivity of the brackish, saline and hyper saline water samples were determined using EC meter. The water samples were kept in flask for desalination experiments.

The desalination experiment was carried out using a suction pump, a Buchner funnel, the prepared membrane, and a filter paper. The suction pump has 0.5hp power rating, Mode 2 x 2^{-4A}, free air displacement of 8cfm, ultimate vacuum of 3 x 10⁻¹ Pa, and voltage of 220V/50Hz. The ion separation efficiencies of the fabricated graphene membrane for brackish, saline and hyper-saline water was investigated by passing each of the water samples through the membrane for a total time of 150 minutes each, and the conductivity of the filtered water was taken at an interval of 30 min.

RESULTS AND DISCUSSION

Properties of Graphene Material and Graphene Membrane

The morphology of the graphene/graphene oxide nanomaterial as acquired by transmission electron microscopy is shown in Figure 1. Layers of large-area graphene sheets produced via electrochemical exfoliation are evident from the TEM images. The SEM/EDX spectrum of the graphene nanomaterials confirms a carbon-based material, with the presence of C, O, Si, and Cl in the graphene nanomaterials. The presence of oxygen in the EDX could suggest an oxidized form of graphene material. Hydrochloric acid used in pretreatment washing of electrodes, or potassium chlorate used as electrolyte may have introduced chlorine into the graphene sample. Silicon may have been introduced from the original battery electrodes or in the sample preparation for SEM/EDX analysis. The quantitative EDX elemental analysis showed the atomic percentage of all elements present in the sample as C – 87.52%, O – 11.70%, Si – 0.11%, and Cl – 0.66%. The EDX elemental composition gives a mass-content ratio of carbon to oxygen atoms (C/O ratio) in the graphene as 7.48, indicating the high content of oxygen functional groups in the sample.

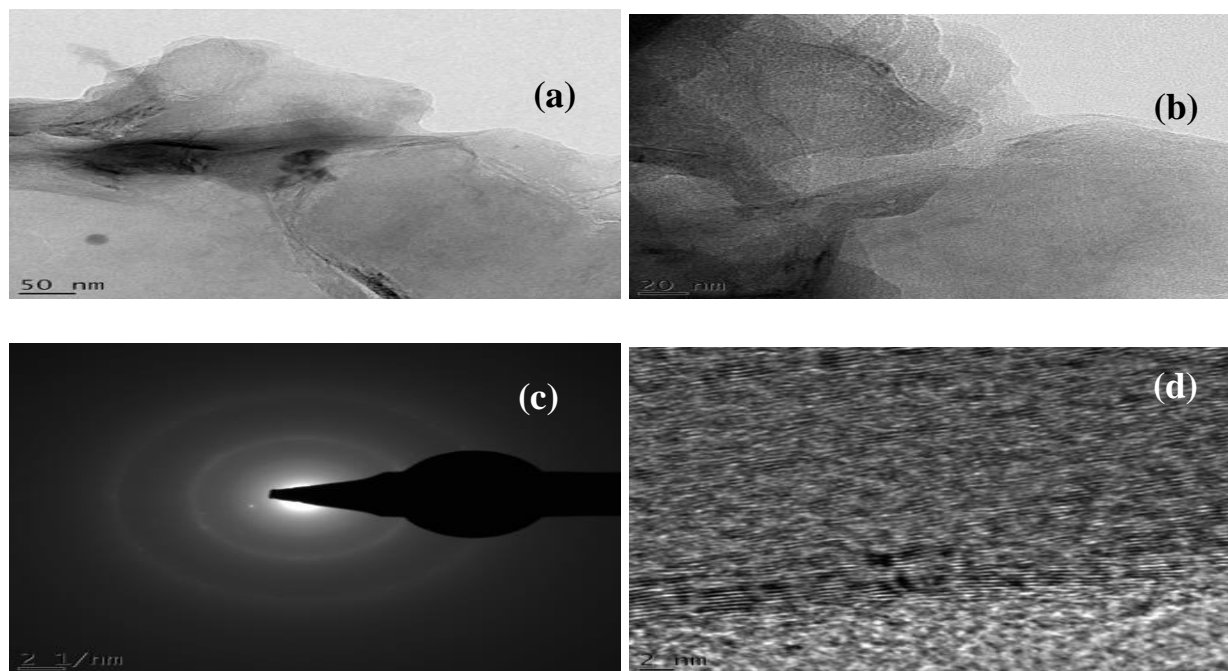


Figure 1 TEM images of graphene/graphene oxide produced from electrochemical exfoliation of ZCBs showing (a),(b) evidence of few-layer graphene nanomaterial, (c) the SAED pattern, and (d) lattice fringes/arrangement of carbon atoms in the graphene sheet.

Figure 2 shows the UV-Visible absorbance spectra of the graphene nanomaterials produced at different electrochemical exfoliation conditions of applied voltage. The spectra show absorption peaks were observed between 264 and 258 nm for the samples produced at different voltage values, which are indicative of graphene nanomaterial.

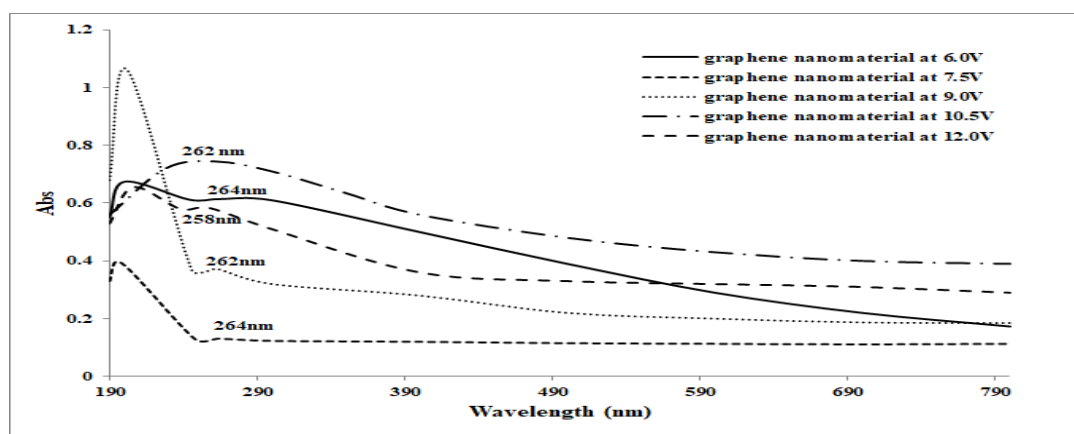


Figure 2 The UV-visible spectra of graphene nanomaterials produced from electrochemical exfoliation of ZCBs

The FTIR spectrum of the graphene nanomaterial was obtained (Figure not shown). The presence of different types of oxygen functionalities in graphene oxide were confirmed by three distinct peaks at 3455.41 , 2090 , and 1634cm^{-1} . The peak at 3455.41cm^{-1} is characteristic stretching vibration mode for graphene oxide, OH groups from C–OH group or water molecule (Rattana *et al.*, 2012; Tucureanu *et al.*, 2016). The peak at 2090cm^{-1} could be due to SiC fake diamond which occurs in the $1200\text{-}2400\text{cm}^{-1}$ region (Tucureanu *et al.*, 2016). The EDX result may have also suggested the likely presence of SiC in the sample. The peak at 1634cm^{-1} could be assigned to

different structures of carbon-based materials such as carbon quantum dots (CQDs) in a complex, a skeletal ring in CQD formed from graphite or graphene, or skeletal ring in CQDs (Tucureanu *et al.*, 2016). It could also indicate skeletal polycyclic aromatic hydrocarbons in CQD formed from graphite or graphene, the OH groups from water molecule (H_2O) in graphite, or the $\nu(C = C)$ in diamond-like carbon films (amorphous carbon) (Tucureanu *et al.*, 2016). Also, it could be assigned to C=O stretching of carboxylic and/or carbonyl moiety functional groups (Rattana *et al.*, 2012). More so, it has been reported to be due to graphene oxide, attributable to O-H vibrations of water (Manorathne *et al.*, 2017).

The HRSEM images of the graphene-cellulose composite membrane are presented in Figure 3(a)–(e), and its digital picture (f). It can be observed from Figure 3(a)–(c) that the membrane is porous, property that would make it permeable to fluid. It has characteristic multimodal pore size distributions that are interstitial, which should be well suited for ion retention of small molecules.

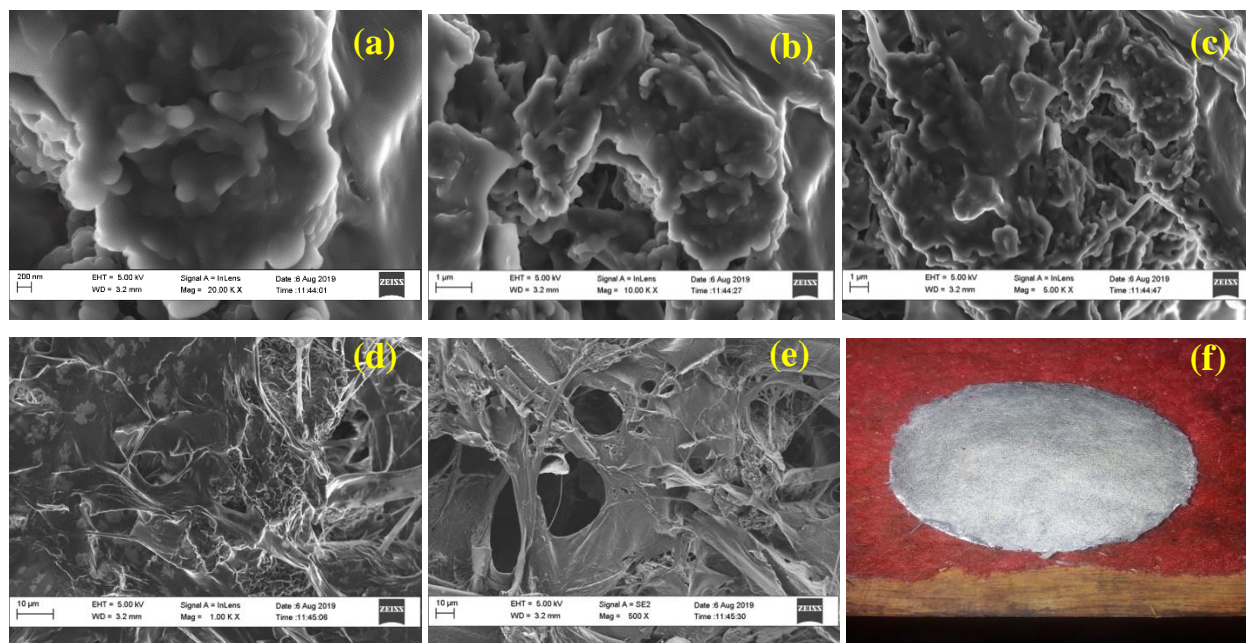


Figure 3 (a)-(e) HRSEM images of graphene-cellulose membrane, (f) its digital picture.

Also, the morphological images show that the cellulosic structure of paper pulp used as support was retained in the mix (Figure 3(e)), and graphene nanoparticles were well incorporated into the support matrix (Figure 3(d)). The SEM/EDX elemental compositions of the showed that the membrane is composed of elements similar to that of the starting graphene and cellulose paper material. For example, the elements (C, O, Si and Cl) found in the original graphene material are also present in the composite membrane. In addition, Ca, Al, and K are present which could be from the cellulose paper pulp. Some of the elements – aluminum, silicon, calcium, and potassium are common with kaolin, which is a constituent in cellulose papers usually added in small quantity to improve the whitening. Kaolin is an alumino-silicate material that could contain other elements in varying amounts depending on its source. The atomic percent of elements in the graphene-cellulose membrane was found as: C – 71.29%, O – 28.08%, Al – 0.13%, Si – 0.21%, Cl – 0.09%, K – 0.06%, and Ca – 0.15%, showing carbon and oxygen as the main constituents of cellulose. The carbon composition in the graphene-cellulose composite membrane is lower than in graphene oxide because cellulose is composed of relatively higher oxygen than the oxidized graphene. The membrane swelling ratio, calculated using Equation (1) was found to be 46.33%. The weight of the membrane after its immersion in water for 6 hr was 0.578g, and its weight after drying was taken to be 0.395g. By Equation (1);

$$Swelling\ ratio = \frac{M_{wet} - M_{dry}}{M_{dry}} \times 100 = \frac{0.578 - 0.395}{0.395} \times 100 = 46.33\%$$

The salt water flux (SWF) depends on the porous nature of the membranes. A better SWF will be obtained in a porous membrane structure. Permeation studies were carried out in a suction filtration setup. The results of permeation property of the graphene-cellulose membrane tested by SWF experiment, at different salt concentrations, are shown in Table 1. Effective membrane area was

calculated to be 0.001735 m^2 (dia. 47 mm). The flux experiments were carried out at ultimate vacuum of 0.3Pa. This was observed consistently, and hence, concluded based on the SWF values in Table 1 that the membrane is hydrophilic in nature and has a transitional good flow rate, flux rate and permeability. The average volumetric flow rate, flux, and permeability of the membrane were therefore obtained as $6.5285 \times 10^{-5} \text{ m}^3/\text{m}^2 \cdot \text{s} \cdot \text{Pa}$, $1.9585 \times 10^{-5} \text{ m}^3/\text{m}^2 \cdot \text{s}$, and $3.3985 \times 10^{-6} \text{ m}^3/\text{s}$ respectively.

Table 1 The membrane flow rate, flux and permeability observed for different salty water types

	Brackish	Saline	hyper-saline
Surface area (m^2)	0.001735	0.001735	0.001735
Flow rate (m^3/s)	3.400×10^{-6}	3.377×10^{-6}	3.420×10^{-6}
Flux ($\text{m}^3/\text{m}^2 \cdot \text{s}$)	1.959×10^{-5}	1.946×10^{-5}	1.971×10^{-5}
Permeability ($\text{m}^3/\text{m}^2 \cdot \text{s} \cdot \text{pa}$)	6.532×10^{-5}	6.487×10^{-5}	6.570×10^{-5}
Vacuum pressure (Pa)	0.3	0.3	0.3

The Membrane Desalination Experiment

The initial conductivities before desalination and final conductivities at the end of 150 min desalination time for the three salty water types are presented in Table 2.

Table 2 Initial and final conductivities before and after 150 min desalination experiment

Salty water type	brackish	saline	hyper-saline
Initial conductivity (mS/cm)	10.76	12.54	16.65
Final conductivity (mS/cm) at 150 min	0.968	1.142	1.168

Conductivity is a function of salt ion concentration in water. In the results as presented in Table 2, it was observed that there was significant reduction in the initial conductivities of the water samples after membrane filtration, which is an indication that the graphene-cellulose composite membrane was effective in the salt ion separation. The initial conductivities of brackish, saline and hyper-saline water dropped from 10.76, 12.45 and 16.65 mS/cm to final values of 0.968, 1.14 and 1.168 mS/cm respectively, after 150 min of suction filtration through the graphene-cellulose membrane at ultimate vacuum pressure of 0.3 Pa.

It was also investigated the change in conductivity of water samples with time as the membrane filtration progressed. The variation results are shown in Figure (4) – (6) for brackish, saline and hyper-saline water.

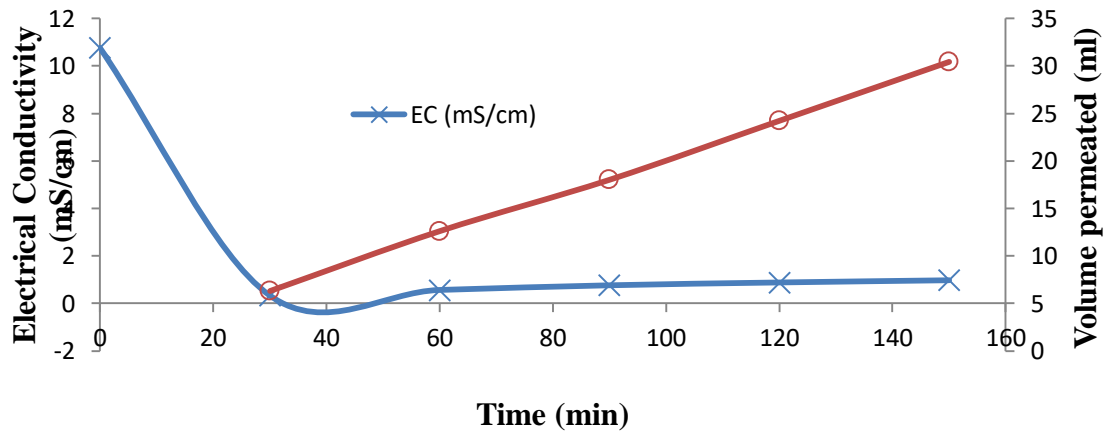


Fig. 4. Variation of conductivity with desalination time in brackish water

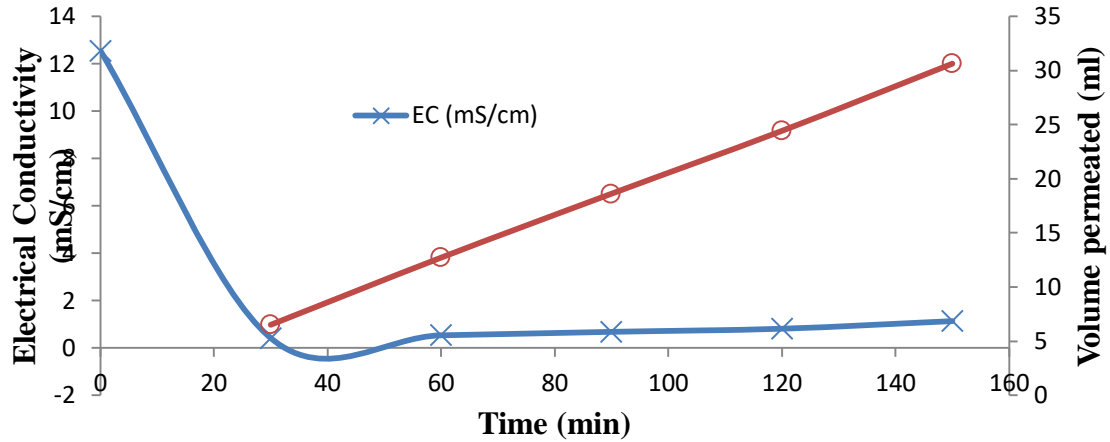


Fig. 5. Variation of conductivity with desalination time in saline water

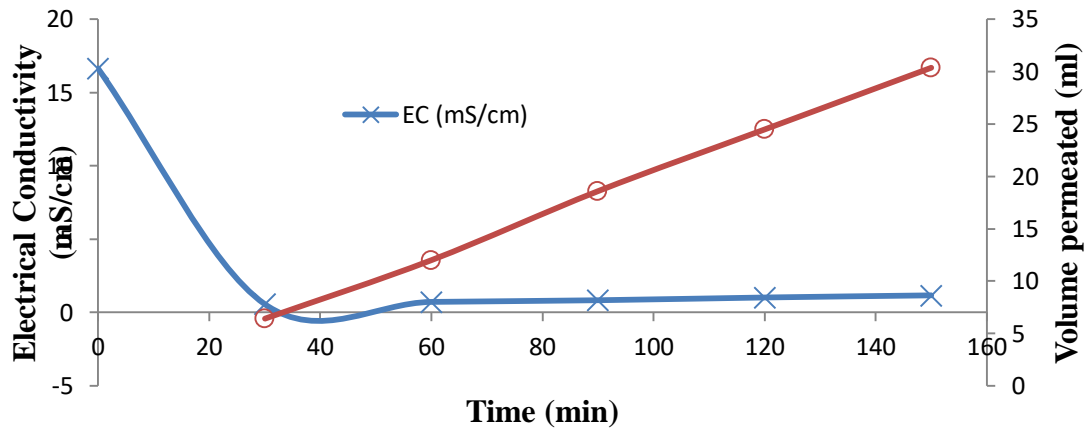


Fig. 6. Variation of conductivity with desalination time in hyper-saline water

The desalination time of 30 min was the optimum in all cases of the membrane filtration. After the initial 30 min had elapsed, it was observed that there was increase in the conductivities of the filtered water with further time, but at a slow rate. This is likely due to swelling of the membrane material that leads to permeation of salt ions to transport through. Cellulose in the membrane is hydrophilic in nature. Swelling of membrane could cause increase in the membrane interlayer spacing, thereby losing the filtration ability for hydrated ions (Yan et al. 2017). However, water flux was constant as there was steady permeation of water through the porous membrane which can be observed from the graphs of volume of water permeated with time in

Figures (4) – (6). It is the authors understanding that the graphene oxide-cellulose membrane has potential in filtration processes as demonstrated in the three experiments.

CONCLUSION

The study demonstrated the possibility of producing low-cost graphene oxide-cellulose membrane from waste materials of zinc-carbon batteries and waste papers. It was also shown that the graphene oxide-cellulose membrane has the potential for water desalination and other forms of ion separation. Characterization results showed that the oxidized graphene nanomaterial prepared by electrochemical exfoliation possessed the desired excellent properties to improve the performance of membrane materials. Surface functional groups in the graphene oxide can serve as ion sieves for the membrane. Overall, the graphene oxide-cellulose composite presented such properties that are adequate for membrane filtration.

ACKNOWLEDGEMENTS

The authors wish to thank the Department of Electrical and Electronics Engineering of University of Ilorin, Nigeria for permitting the use of Laboratory DC Power Supply (MCP Model: M10-SP3003L). The permission granted by the Department of Chemistry of University of Ilorin for the use of UV-Vis spectrophotometer is also acknowledged.

REFERENCES

- Abdel-Shafy H.I. and Mansour M.S.M. 2018. Solid waste issue: Sources, composition, disposal, recycling, and valorization. *Egyptian Journal of Petroleum* 27: 1275–1290. <https://doi.org/10.1016/j.ejpe.2018.07.003>
- Anis S.F., Hashaikeh R. and Hilal N. 2019. Functional materials in desalination: A review. *Desalination* 468: 114077. <https://doi.org/10.1016/j.desal.2019.114077>

- Chen C., Jia L., Li J., Zhang L., Liang L., Chen E., Kong Z., Wang X., Zhang W. and Shen J-W. 2020. Understanding the effect of hydroxyl/epoxy group on water desalination through lamellar graphene oxide membranes via molecular dynamics simulation. *Desalination* 491:114560. <https://doi.org/10.1016/j.desal.2020.114560>
- Colburn A., Wanninayake N., Kim D.Y. and Bhattacharyya D. 2018. Cellulosegraphene quantum dot composite membranes using ionic liquid. *Journal of Membrane Science* 556: 293–302. <https://doi.org/10.1016/j.memsci.2018.04.009>
- Ezeudu O.B., Agunwamba J.C., Ezeasor I.C. and Madu C.N. 2019. Sustainable Production and Consumption of Paper and Paper Products in Nigeria: A Review. *Resources* 8(53): 1-23. [Doi:10.3390/resources8010053](https://doi.org/10.3390/resources8010053)
- Hayes W.I., Joseph P., Mughal M.Z. and Papakonstantinou P. 2014. Production of reduced graphene oxide via hydrothermal reduction in an aqueous sulphuric acid suspension and its electrochemical behavior. *J Solid State Electrochem* 1-20. [DOI 10.1007/s10008-014-2560-6](https://doi.org/10.1007/s10008-014-2560-6)
- Koga H., Tonomura H., Nogi M., Suganuma K., and Nishina Y. 2016. Fast, Scalable, and Eco-Friendly Fabrication of Energy Storage Paper Electrode. *Green Chemistry* 2015: 1-22. [DOI: 10.1039/C5GC01949D](https://doi.org/10.1039/C5GC01949D).
- Lin L., Deng B., Sun J., Peng H., and Liu Z. 2018. Bridging the Gap between Reality and Ideal in Chemical Vapor Deposition Growth of Graphene. *Chemical Reviews* 118: 9281–9343. [DOI: 10.1021/acs.chemrev.8b00325](https://doi.org/10.1021/acs.chemrev.8b00325)
- Manorathne C.H., Rosa S.R.D, and Kottegoda I.R.M. 2017. XRD-HTA, UV Visible, FTIR and SEM Interpretation of Reduced Graphene Oxide Synthesized from High Purity Vein Graphite. *Material Science Research India* 14(1): 19-30. <http://dx.doi.org/10.13005/msri/140104>

Rattana T., Chaiyakun S., Witit-anun N., Nuntawong N., Chindaudom P., Oaew S., Kedkeaw C., and Limsuwan P. 2012. Preparation and characterization of graphene oxide nanosheets. *Procedia Engineering* 32: 759 – 764. [doi:10.1016/j.proeng.2012.02.009](https://doi.org/10.1016/j.proeng.2012.02.009)

Sahoo S.K., Behera A.K., Chandran R., Mallik A. 2020. Industrial scale synthesis of few- layer graphene nanosheets (FLGNSs): an exploration of electrochemical exfoliation approach. *Journal of Applied Electrochemistry* 1-16. <https://doi.org/10.1007/s10800-020-01422-3>

Song N., Gao X., Ma Z., Wang X., Wei Y. and Gao C. 2018. A review of graphenebased separation membrane: Materials, characteristics, preparation and applications. *Desalination* 437: 59–72. <https://doi.org/10.1016/j.desal.2018.02.024>

Su C-Y., Lu A-Y., Xu Y., Chen F-R., Khlobystov A.N. and Li L-J. 2011. High quality thin graphene films from fast electrochemical exfoliation. *ACS nano* 5(3): 2332-2339.

Teow Y.H. and Mohammad A.W. 2017. New generation nanomaterials for water desalination: A review. *Desalination*. <https://doi.org/10.1016/j.desal.2017.11.041>

Țucureanu V., Matei A., and Avram A.M. 2016. FTIR Spectroscopy for Carbon Family Study. *Critical Reviews in Analytical Chemistry* 46(6): 502-520. DOI: [10.1080/10408347.2016.1157013](https://doi.org/10.1080/10408347.2016.1157013)

Yang Z., Ma X-H., and Tang C.Y. 2017. Recent development of novel membranes for desalination. *Desalination*. <https://doi.org/10.1016/j.desal.2017.11.046>

Zhang L., Dai F., Yi R., He Z., Wang Z., Chen J., Liu W., Xu J. and Chen L. 2020. Effect of physical and chemical structures of graphene oxide on water permeation in grapheme oxide membranes, *Applied Surface Science*. <https://doi.org/10.1016/j.apsusc.2020.146308>

Zhong Y., Mahmud S., He Z., Yang Y., Zhang Z., Guo F., Chen Z., Xiong Z., and Zhao Y. 2020. Graphene oxide modified membrane for highly efficient wastewater treatment by dynamic

combination of nanofiltration and catalysis. *Journal of Hazardous Materials*

<https://doi.org/10.1016/j.jhazmat.2020.122774>